Journal of Materials Chemistry C

Robust fluorescent calcium coordination polymers as Cu2+ sensors with high sensitivity and fast response

Journal:	*Journal of Materials Chemistry C*
Manuscript ID	TC-ART-02-2020-000825.R1
Article Type:	Paper
Date Submitted by the Author:	28-Mar-2020
Complete List of Authors:	Wu, Zhao-Feng; Fujian Institute, Velasco, Ever; Rutgers University Shan, Chuan; University of South Florida Tan, Kui; University of Texas at Dallas, Department of Materials Science and Engineering Zhang, Zhi-Zhuan; Fujian Institute of Research on the Structure of Matter Hu, Qianqian; Fujian Institute of Research on the Structure of Matter, Chinese Academy of Sciences, Xing, Kai; Harbin Institute of Technology, Department of Chemistry Huang, Xiao-ying; Fujian Institute of Research on the Structure of Matter, Li, Jing; Rutgers The State University of New Jersey, Chemistry and Chemical Biology

Journal Name

ARTICLE

Robust fluorescent calcium coordination polymers as Cu^{2+} sensors with high sensitivity and fast response

Received 00th January 20xx,
Accepted 00th January 20xx

DOI: 10.1039/x0xx00000x

www.rsc.org/

Zhao-Feng Wu,[a,b,#] Ever Velasco,[a,#] Chuan Shan,[c] Kui Tan,[d] Zhi-Zhuan Zhang,[b] Qian-Qian Hu,[b] Kai Xing,[e] Xiao-Ying Huang[b,*] and Jing Li [a,*]

A three-dimensional (3D) and highly fluorescent calcium-based coordination polymer (Ca-CP) has been synthesized and structurally characterized. Built on a strongly fluorescent (FL) chromophore ligand, $[Ca(H_2tcbpe)(H_2O)_2]$ (**1**) (H_4tcbpe = 4', 4''', 4''''', 4'''''''-(ethene-1,1,2,2-tetrayl) tetrakis(([1,1'-biphenyl]-4-carboxylic acid)) is highly luminescent. Photoluminescence (PL) studies indicate that **1** undergoes a bathochromic shift in emission energy from blue to green color upon outgassing or under mechanic force. Notably, **1** exhibits selective FL sensing for Cu^{2+} ions with a detection limit (LOD) of 0.064 ppm, far below the U.S. WHO and EPA standard for drinking water. Detailed investigation of the sensing mechanism reveals that uncoordinated COO^- groups in **1** play a major role in recognizing Cu^{2+} ions. This is supported through analysis by multiple characterization methods including IR, EDS and XPS. Based on the proposed mechanism, an isostructural $[Ca(H_2tcbpe\text{-}F)(H_2O)_2]$ Ca-CP (**2**) (H_4tcbpe-F = 4', 4''', 4''''', 4'''''''-(ethene-1,1,2,2-tetrayl)tetrakis(3-fluoro-[1,1'-biphenyl]-4-carboxylic acid)) is synthesized and tested. Compound **2** demonstrates a ten-fold enhancement in Cu^{2+} detection sensitivity with a ppb level detection limit. The strong enhancement in the detection sensitivity results from optimized electron density around free COO^- groups by introducing electron withdrawing F groups onto the backbone of the organic linker. Excellent chemical stability under a wide range of pH conditions (1-14), high sensitivity and rapid fluorescence quenching response time (seconds) make these compounds ideal candidates for use as Cu^{2+} sensors.

1. Introduction

As a ubiquitous and relatively abundant metal, copper (Cu) is an essential element in all living organisms and has been widely used in the development of human society.[1] However, excessive Cu^{2+} may be harmful for the ecosystem and even threaten human health.[2] The World Health Organization (WHO) and the United States Environmental Protection Agency (EPA) require Cu^{2+} concentration in drinking water to be below 2 and 1.3 ppm, respectively.[3] Thus, great efforts have been made to sensitively detect Cu^{2+} ions. Traditional methods, e.g. inductively coupled plasma mass spectrometry (ICP-MS), atomic absorption spectroscopy (AAS), and electrochemical methods are commonly used for detecting Cu^{2+}.[4] However, the expensive instruments, long data-acquisition time and the necessity of technical professionals are key limitations that hinder the popularization of these methods especially in underdeveloped countries and regions. Therefore, as a comparatively simple and inexpensive method with short response time, fluorescent (FL) sensing based on luminescent materials serves as a facile, convenient alternative to detect Cu^{2+}.[5]

In the past two decades, as a new type of FL material, metal organic framework (MOF) or coordination polymer (CP) based luminescent sensors have been developed for the detection of metal ions, toxic molecules, temperature, and so on.[6] Recent advances in the FL detection of Cu^{2+} ions allow for the rapid and sensitive detection, however the chemical instability of many of these compounds in aqueous environment limit studies largely to organic solvents.[7] Thus, there remains a strong need to design FL MOF/CP-based probes that have improved stability in aqueous environments while retaining a rapid, sensitive FL response towards Cu^{2+}.

Herein, a three-dimensional (3D) FL CP formulated as $[Ca(H_2tcbpe)(H_2O)_2]$ (**1**) has been assembled from Ca^{2+} and an aggregation induced emitting (AIE) ligand 4', 4''', 4''''', 4'''''''-(ethene-1,1,2,2-tetrayl) tetrakis(([1,1'-biphenyl]-4-carboxylic

[a] Department of Chemistry and Chemical Biology, 123 Bevier Rd. Piscataway, NJ 08854, United States
[b] Fujian Institute of Research on the Structure of Matter, the Chinese Academy of Sciences, Fuzhou, Fujian, 350002, P.R. China
[c] Department of Chemistry, University of South Florida, 4202 E. Fowler Avenue, Tampa, FL 33620, USA.
[d] Department of Materials Science & Engineering, University of Texas at Dallas, Richardson, Texas 75080, USA.
[e] Harbin Institute of Technology, No.92 Xidazhi Street Nangang District, Harbin, 150006, P.R. China
[#] The authors contributed equally.
E-mail: jingli@rutgers.edu
Electronic Supplementary Information (ESI) available: PXRD patterns, more crystal structural details, PL spectra, TG profiles. CCDC 1950587. For ESI and crystallographic data in CIF or other electronic format see DOI: 10.1039/x0xx00000x.

acid)) (H_4tcbpe). Compound **1** exhibits an interesting solvent-dependent FL property whereby dispersion of **1** in solvents with varying polarity tunes its multicolour emission. Notably, when solutions containing Cu^{2+} ions were introduced to competitively bind with protons to interrupt the H-bonded network in **1,** sensitive "turn off" FL occurs within seconds. The mechanism was investigated by multiple techniques including but not limited to IR, EDS and XPS. Based on the sensing mechanism, an isostructural compound with molecular formula [Ca(H_2tcbpe-F)(H_2O)$_2$] (**2**) was designed by introducing a F^- functionalized form of the ligand 4', 4''', 4''''', 4'''''''-(ethene-1,1,2,2-tetrayl)tetrakis(3-fluoro-[1,1'-biphenyl]-4-carboxylic acid) (H_4tcbpe-F). As anticipated, the sensing sensitivity of **2** towards Cu^{2+} cations is further enhanced, showing an improvement of nearly ten-fold in the detection sensitivity compared to **1**. Lastly, the excellent chemical stability in harsh aqueous environments (pH 1-14), coupled with rapid and sensitive FL response make both titled compounds ideal candidates as FL probes for the detection of Cu^{2+} ions.

2. Experimental

2.1 Materials and methods

Powder X-ray diffraction patterns were recorded on a Rigaku Ultima IV with Cu Kα radiation (λ = 1.5406 Å). Data were collected at room temperature at 2θ = 3-40° with a scan speed of 2°/min and operating power of 40 kV and 44 mA. Thermogravimetric data were collected on a TA Q5000 Analyzer with a temperature ramping rate of 10 °C/min from room temperature to 700 °C under nitrogen gas flow. The solid-state emission spectra of the title compounds were recorded by a Duetta fluorescence and absorbance spectrometer at room temperature. The quantum yields were recorded on an Edinburgh FLS920 fluorescence spectrometer at room temperature. The single crystal X-ray diffraction data of **1** was collected with graphite-monochromated CuKα (λ = 1.54178 Å) using a Bruker D8 Venture PHOTON II CPAD at 150 K. Energy dispersive spectroscopy (EDS) was obtained with a JEOL JSM-6700F scanning electron microscope. The IR spectroscopic data were obtained using a Nicolet 6700 Fourier transform IR spectrometer. X-ray photoelectron spectroscopy (XPS) measurements were performed using an ESCALAB 250Xi X-ray Photoelectron Spectrometer (XPS) Microprobe.

2.2 Synthesis of MOFs:

Synthesis of 1: A mixture of Ca(ClO_4)$_2$·6H_2O (50 mg, 1 mmol), H_4tcbpe (20 mg) in formic acid (0.5 mL), DMF (5 mL) and H_2O (2 mL) was sealed in a 20 mL glass vial and heated in 120 °C oven for 2 days. Colorless flake crystals of **1** (30% yield based on calcium) were obtained after ethanol washing, Fig. S1.

Synthesis of 2: A mixture of Ca(ClO_4)$_2$·6H_2O (50 mg), H_4tcbpe-F (20 mg) and benzoic acid (50 mg) in DMF (5 mL) and H_2O (2 mL) was sealed in a 20 mL glass vial at 393K for 2 days. Light yellow flake crystals (35% yield based on calcium) were obtained after ethanol washing, Fig. S2.

2.3 Fluorescence measurements

The as-made crystalline samples (**1** or **2**) were loaded into an agate mortar and manually ground using a mortar and pestle to obtain fine powders. The FL spectra of these samples were then recorded in solutions prepared by dispersing 2 mg of sample in either 2 mL of a given organic solvent or 2 mL solution of 10^{-4} M metal ion solutions. After ultrasonication, the suspension was placed in a quartz cell of 1 cm width for FL detection. FL detection experiments were conducted by preparing ultrasonication induced suspensions of **1** or **2** (2 mg) in 2 mL of DI water. To the resulting suspensions was injected the various concentrations of either H^+ or Cu^{2+} ions. A stopwatch was used to record the time in order to make the FL detection accurate and reproducible. The PL data were collected after 5 seconds after the analyte was added into the quartz cell. For all the measurements, the dispersed emulsions of **1** and **2** were excited at 350 nm and 380 nm while monitoring the corresponding emission wavelengths from 400 nm to 700 nm.

2.4 X-ray crystallography

Crystals of **1** suitable for single crystal X-ray diffraction (SCXRD) were selected under an optical microscope and glued to a thin glass fiber. After data collection, the structure was solved by direct methods and refined with full-matrix least squares techniques using the *SHELX2016* package.[8] The detailed crystallographic data and structure-refinement parameters are summarized in Table 1. The structure was deposited in Cambridge Structural Database (CSD) and the CCDC number is 1950587.

Table 1 Crystallographic data and structural refinement details for **1**.

Empirical formula	$C_{54}H_{38}CaO_{10}$
Crystal Size (mm)	0.12 x 0.07 x 0.04 mm
Crystal system	monoclinic
Space group	*C*2/*c*
a (Å)	46.0700(16)
b (Å)	7.8309(3)
c (Å)	12.0264(4)
β (°)	103.8640(10)
V (Å^3)	4212.4(3)
Z	4
μ (mm^{-1})	1.825
λ(Cu*K*α) (Å)	1.54178
F(000)	1848
θ range (°)	3.953 to 74.698
Reflections measured	20252
Independent reflections	4186
Temperature (K)	150(2)
ρ_{calc}/g cm^{-3}	1.399
Parameter	311
R_{int}	0.0355

R_1, wR_2 $[I>2\sigma(I)]^a$	0.0356, 0.0891
R_1, wR_2 [all data]	0.0383, 0.0914
GOF	1.067
Largest diff. Peak and hole/e Å^{-3}	0.208 and -0.352

$^aR_1 = \sum \| F_o | - | F_c \| / \sum | F_o |$. $^bwR_2 = [\sum w(F_o^2 - F_c^2)^2 / \sum w(F_o^2)^2]^{1/2}$

3. Results and discussion

3.1 Crystal structure description

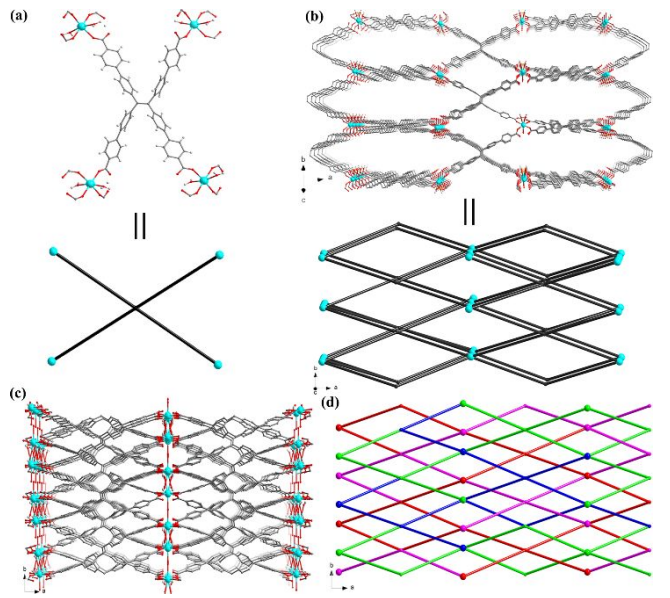

Fig. 1 (a) Coordination geometry of the tcbpe ligand and Ca^{2+} in **1**. (b) Single Ca-tcbpe 4,4-connected net along the [001] direction. (c) The 3 D framework of **1** viewed from the crystallographic *c* axis. (d) Line connectivity drawing showing the 4-fold interpenetration of the Ca-tcbpe nets.

Single crystal X-ray diffraction analysis indicates that **1** crystallizes in the space group *C*2/*c* and the asymmetric unit contains half of the formula unit. In compound **1**, Ca^{2+} adopts a six-coordinated distorted octahedral geometry, where the equatorial plane is surrounded by four carboxylates from four different H_4tcbpe linkers through a monodentate coordination mode while the two apical positions coordinate to two terminal water molecules. Each H_4tcbpe ligand is only half deprotonated and connects to four Ca^{2+} ions with its four carboxylate groups (Fig. 1a). Interconnections of ligands via Ca^{2+} ions result in a three-dimensional (3D) framework (Fig. 1b). Considering H_4-tcbpe as a distorted 4-c node with respect to linker connectivity, the 3D structure may be simplified as a 4,4 connected network. Topological analysis through the ToposPro Database reveals that **1** belongs to the known *pts* topology with the point symbol $\{4^2 \cdot 8^4\}$, Fig. 1d. The large linker size and degree of flexibility result in a 4-fold interpenetrated framework containing four of these identical nets (Fig. 1c). In addition to the hydrogen bonding that exists between the uncoordinated carboxylic oxygen atom and H^+, there are additional hydrogen bonds between the terminal water and uncoordinated oxygen atom from COO^- groups that further stabilize the framework (Fig. S4 and Table S1).

3.2 FL sensing properties

Solid state FL spectra indicates that as-made **1** emits blue centered emission at 425 nm under 350 nm excitation, as shown in Fig. 2. Interestingly, **1** exhibits a mechanoresponsive bathchromic shift in FL emission after grinding, shifting from a blue to green emission centered at 525 nm (inset of Fig. 2 and Fig. S6a). After immersing the power sample in DMF or DMA overnight, its FL turns back to blue emission, indicating the mechanochromism behavior of **1** is reversible. The quantum yields (QYs) of **1** are 84.86% and 60.82% before and after grinding, respectively. When dispersed in various solvents (e.g. DMF, DMA, ethanol and acetone) powdered **1** showed solvents dependent FL (Fig. S6b). But the intensity is much lower than that of the solid state FL, indicating the compound also exhibits AIE behavior as in the case of the ligand. The emission of as-made **1** undergoes the same effect after being exposed to a temperature of 200 to 400 °C under N_2 atmosphere for 2 hours (Fig. S7). The powder X-ray diffraction (PXRD) patterns indicate there is no discernible difference between the as-made and ground or thermally-activated samples, suggesting no occurrence of crystal phase transition before and after grinding or heating (Fig. S3 and Fig. S8). As H_4tcbpe is a typical AIE emitting ligand with abundant benzene rings, FL of such ligands is usually sensitive to external factors that results in the release of twisting stress and/or rupturing of the noncovalent interactions of the ligand that can induce such mechanochromic and thermal induced tunable FL behaviour.[9]

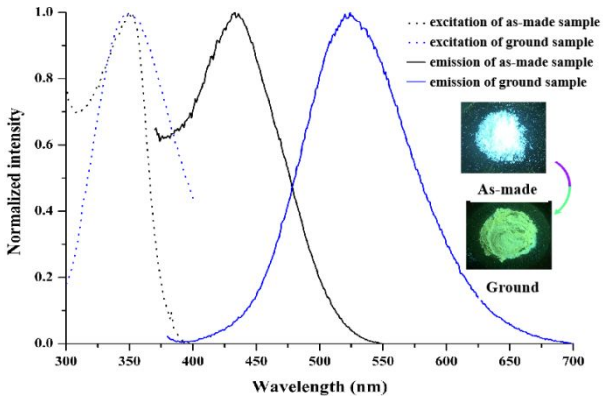

Fig. 2 Solid state FL spectra of as-made crystals of **1** before and after grinding. Insets show photographic images of the luminescent changes of **1** at room temperature under 365 nm excitation.

The chemical stability of **1** was determined by immersing ground samples in aqueous solutions ranging from pH 1 to 14 for more than 24 hours; the resulting PXRD patterns reveal practically no loss of crystallinity (Fig. 3). Compound **1** features a compact structure owing to a 4-fold interpenetration of framework. Within the structure, the tcbpe ligand is well confined by coordinating to Ca^{2+} ions and forming strong hydrogen bonding with carboxylic groups of other tcbpe ligands and terminal water molecules (Fig. S4). Thus, the competitive coordination interaction between guests or ions (e.g. H_2O and OH^-) and COO^- group with Ca^{2+} is reduced in some extent. In **1**, each H_4tcbpe ligand is only half deprotonated, and the

electrostatic repulsion presents between the skeleton and H^+, therefore keeping the labile metal-ligand bonds from being attacked. These reasons may explain why the framework remains stable in the presence of acidic/alkaline aqueous media.[10] The excellent stability of **1** in water encouraged us to further investigate potential FL sensing applications in harsh aqueous conditions. From a structural perspective, the H_4tcbpe ligand in **1** is half pronated and the intermolecular H-bond network constructed from the COO^- groups, protons and water molecules (Fig. S4), implies that it may be possible for other cations to undergo competitive binding with this network that may result in alterations in the FL signal of the framework. We exposed finely ground powders of **1** into H_2O with various pH conditions from 1 to 14 and monitored the resulting impact that pH imposed on the emission spectra of **1**. As depicted in Fig. S9, when dispersed in an acidic pH 1 solution, **1** emits bright green emission centered at 519 nm, while emission profile in the pH range of 3-10 remains similar, shifting the pH to a value of 14 produces a significant blue-shift in emission of about 50 nm. Notably, **1** undergoes a significant, uncommon "turn-on" behavior upon addition of the pH 1 solution into the emulsion of **1** (Fig. S10). The original fluorescence of **1** undergoes an emission enhancement of more than 2 times of its initial intensity upon exposure to 25 µL of a pH 1 solution. These two observations in the pH dependent luminescence of **1** directly suggests that the local changes induced in the hydrogen bonded framework by varying concentration of H^+ indeed play a major role in tuning the FL of **1**. Thus, we sought to explore if competitive binding with metal cations can disrupt the H-bond network in **1** so that it may serve as a FL sensor for cations.

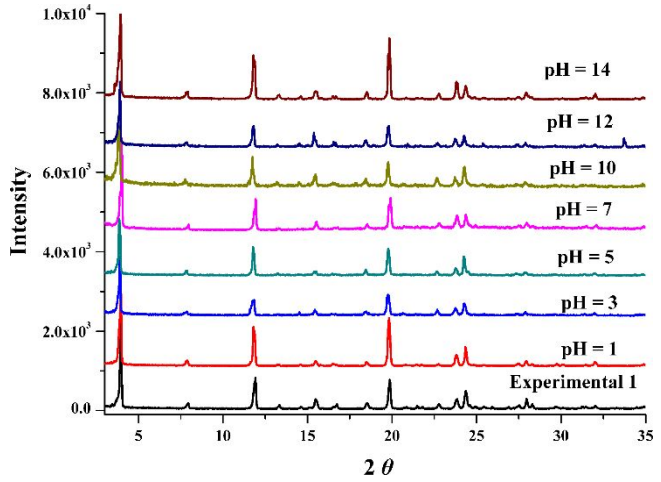

Fig. 3 PXRD patterns of ground sample of **1** under different pH conditions for 24 h.

We then tested the FL response of ground **1** for metal ions by dispersing a powered form of it in 10^{-3} M solutions of various metal salts of the type $M(NO_3)_n$ (M = Li^+, Na^+, K^+, Mg^{2+}, Ca^{2+}, Sr^{2+}, Zn^{2+}, Cd^{2+}, Ni^{2+}, Pb^{2+}, Cu^{2+}, Al^{3+}, Fe^{3+}). Although **1** demonstrates various degree of FL intensity changes towards different metal cations, the most significant and obvious FL quenching response was observed in the case of Cu^{2+}. As seen in Fig. 4, the FL signal quenches gradually as a function of increasing Cu^{2+} concentration, and by more than 60% when as little as 7.5 µM Cu^{2+} was added. Stern-Volmer (SV) analysis reveals that **1** has a K_{sv} value of 1.56×10^5 calculated using the SV equation ($I_0/I = 1 + K_{sv}[M]$,[11] inset of Fig. 4). Accordingly, we can extrapolate the detection limit (LOD) to be 0.064 ppm for Cu^{2+} obtained from the ratio of 3 δ /slope, in which δ is the standard deviation of FL intensity of the blank solution.[12] This value is far below the regulatory limit of Cu^{2+} in drinking water required by U.S. WHO and EPA.[3] This LOD for the detection Cu^{2+} is below most of the previously reported Cu^{2+} FL sensing CPs (Table S2). Furthermore, the FL quenching response of **1** is very fast, and can be achieved within seconds, faster than most of the reported CPs based Cu^{2+} sensors (Table S2). Notably, the outstanding stability of **1** in aqueous environments, whether basic or acidic, and the rapid FL response time place **1** among the best candidates for the detection of Cu^{2+} in aqueous systems.

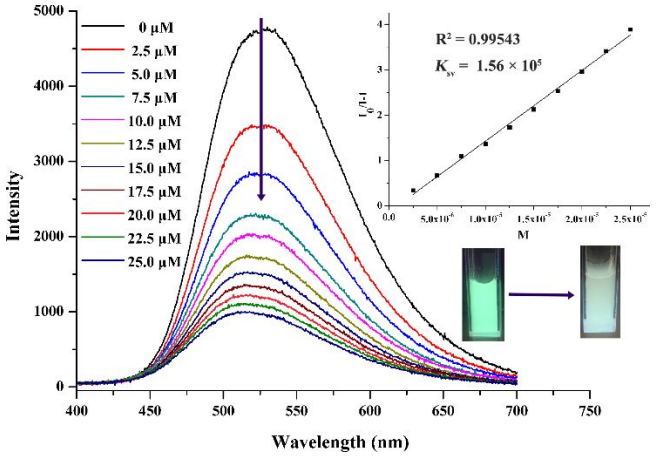

Fig. 4 FL spectra of **1** upon addition of various amounts of 10^{-3} M Cu^{2+} (pH = 7 and response time within 10 s). Inset is the K_{sv} curve for the quenching of **1** by Cu^{2+} and photographs before and after the addition of Cu^{2+}.

We also noted that the degree of FL quenching of **1** in Cu^{2+} solutions is dependent on the pH. The Cu^{2+} sensing performance of **1** was then tested in various acidic conditions. As depicted in Fig. S12, the FL intensity of **1** dispersed in a solution of pH 1 remains unchanged after Cu^{2+} addition. While in pH 3, the FL intensity begins to decrease after the addition of Cu^{2+}, but the quenching effect was not as obvious as in pH 5 or neutral conditions. This result further indicates that H^+ plays an important role in the Cu^{2+} sensing process and the FL quenching involves the competitive binding between H^+ and Cu^{2+}. For **1**, highly acidic conditions maintain and enhance H-bond interactions between free H^+ and the COO^- group; when the pH value increases, Cu^{2+} out-competes protons and limit their interaction with the free COO^- group resulting in FL quenching of the emulsion.

Based on the results discussed above, decreasing the electron density around the free COO^- groups may weaken the H-bond interactions and facilitate the interaction of Cu^{2+} with the free COO^- groups, which may further enhance the FL sensitivity towards Cu^{2+}. Therefore, we explored this through the use a fluorine functionalized ligand H_4tcbpe-f. Through a similar solvothermal reaction, compound **2**, Ca-tcbpe-F, with a

similar crystal structure to **1** was obtained (Fig. S13). As-made **2** also exhibits excellent water stablity under different pH conditions (Fig. S14). The addition of F group to tcbpe may give rise to a higher degree of steric hindrance in **2** which affects the torsional strain between the benzene rings. Thus, although as-made **2** exhibits similar mechanoresponsive FL as **1**, the shift in its emission energy is less significant than **1**, from green to yellow-green (~ 50 nm, Fig. S15). Before and after grinding, the QYs of **2** are 14.08% and 12.26%, respectively. Similar to **1**, compound **2** also exhibits a "turn on" FL responsce towards pH 1 solution (Fig. S16). As dipicted in Fig. S17, **2** also shows selective FL quenching behavior towards Cu^{2+}. Following the same FL detection method as **1**, as seen in Fig. 5, the FL intensity of **2** quenches by more than 60% with an ultra low Cu^{2+} concentration of 1.5 µM, suggesting a much more sensitive FL response to Cu^{2+} than **1**. The K_{sv} value was calculated to be 4.39×10^5 (inset of Fig. 5) with a LOD of 8.32 ppb, exhibiting about a ten-fold increase in sensitivity for Cu^{2+} compared with **1**. The modification of the organic ligand with a F group results in a more sensitive probe for the detection of Cu^{2+} ions.

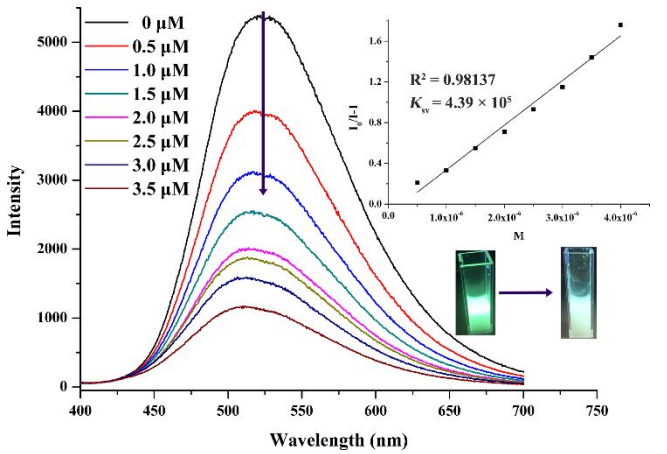

Fig. 5 FL spectra of **2** upon addition of various amounts of 10^{-4} M Cu^{2+} (pH = 7 and response time within 10 s). Inset is the K_{sv} curve for the quenching of **2** by 10^{-4} M Cu^{2+} and the photographs before and after the addition of Cu^{2+}.

To better understand the sensing mechanism, IR, EDS and XPS measurements were conducted. As seen in Figs. S18 and S19, the PXRD patterns of as-made **1** and **2** soaked in high concentrations of 10^{-2} M Cu^{2+} solution are comparable to the experimentally pristine samples, indicating the stability of the titled frameworks. The FTIR spectra of as-made **1** after immersing in 10^{-4} M Cu^{2+} were measured, and the results are plotted in Fig. S20. The characteristic symmetrical stretching bands for the oxygen atoms of the carbonyl at ~1683 cm^{-1} exhibit a modicum of change compared to original **1**. On the other hand, samples of **2** treated in the same concentration of 10^{-4} M Cu^{2+} as **1** result in the characteristic symmetrical stretching band intensity of ~1683 cm^{-1} showing an obvious increase in intensity. This result further indicates that **2** exhibits a more sensitive FL detection ability towards Cu^{2+} compared to **1**. The FTIR spectra suggests that the free carboxylate groups interact with Cu^{2+}, which weaken the intermolecular H-bond interactions between the free carboxylate groups and H^+ thus inducing FL quenching. Treatment of **1** with a low concentration of Cu^{2+} does not alter the IR band intensity around ~1683 cm^{-1}. EDS and XPS measurements were used to further characterize **1** after exposure to Cu^{2+} ions. As shown in Fig. S21, EDS results reveal that Cu^{2+} ions exist within the microcrystals even after washing with copious amounts of H_2O and ethanol indicating that Cu^{2+} forms a strong interaction with **1**. From the XPS measurements, the binding energy of the O 1s peak shifts toward a higher binding energy compared to that of pristine **1** (Fig. S22). Such a shift in binding energy reflects a decrease in electron density suggesting that interactions between the free COO^- group and Cu^{2+} exist.[13] Thus, based on the discussions above, the FL quenching response to Cu^{2+} may be ascribed to the interactions of Cu^{2+} ions with the free oxygen atoms of the carboxylate functional groups of the ligand.

4. Conclusions

In summary, two Ca-based CPs have been synthesized and tested as fluorescent sensing probes for Cu^{2+} ions. The compounds demonstrate ultra-sensitive FL sensing towards Cu^{2+} with a LOD value in the ppm range for **1** and ppb range for **2** after ligand functionalization. The FL quenching mechanism was investigated through multiple experiments and indicates that the FL quench in emission intensity of both compounds results from the interaction between Cu^{2+} and the uncoordinated COO^- groups within the frameworks.

Acknowledgements

This work is partially supported by the U.S. Department of Energy, Office of Science, Office of Basic Energy Sciences under Award No. Award No. DE-SC0019902. Zhao-Feng Wu also acknowledges the support from the China Scholarship Council (CSC).

Conflicts of interest

There are no conflicts to declare.

Notes and references

1 (a) H. Tapiero, D. M. Townsend and K. D. Tew, *Biomed Pharmacother*, 2003, **57**, 386; (b) D. L. de Romana, M. Olivares, R. Uauy and M. Araya, *J. Trace. Elem. Med. Bio.*, 2011, **25**, 3; (c) M. Ebrahimi and M. A. Par, *J. Alloy. Compd.*, 2019, **781**, 1074; (d) F. C. Maier, S. Hocker, S. Schmauder and M. Fyta, *J. Alloy. Compd.*, 2019, **777**, 619.

2 (a) R. P. Csintalan and N. M. Senozan, *J. Chem. Edu.*, 1991, **68**, 365; (b) E. Gaggelli, H. Kozlowski, D. Valensin and G. Valensin, *Chem. Rev.*, 2006, **106**, 1995; (c) H. Kozlowski, A. Janicka-Klos, J. Brasun, E. Gaggelli, D. Valensin and G. Valensin, *Coord. Chem. Rev.*, 2009, **253**, 2665; (d) G. J. Brewer, *Chem. Res. Toxicol*, 2017, **30**, 763.

3 (a) P. G. Georgopoulos, A. Roy, M. J. Yonone-Lioy, R. E.

Opiekun and P. J. Lioy, *J. Toxicol. Env. Heal. B*, 2001, **4**, 341; (b) B. R. Stern, *J. Toxicol. Env. Heal. A*, 2010, **73**, 114.

4 (a) A. C. Liu, D. C. Chen, C. C. Lin, H. H. Chou and C. H. Chen, *Anal. Chem.*, 1999, **71**, 1549; (b) A. P. S. Gonzales, M. A. Firmino, C. S. Nomura, F. R. P. Rocha, P. V. Oliveira and I. Gaubeur, *Anal. Chim. Acta.*, 2009, **636**, 198; (c) D. Walaszek, M. Senn, A. Wichser, M. Faller, B. Wagner, E. Bulska and A. Ulrich, *Spectrochim Acta B*, 2014, **99**, 115; (d) Y. X. Qiu, J. Li, H. B. Li, Q. Zhao, H. M. Wang, H. L. Fang, D. H. Fan and W. Wang, *Sensor Actuat B-Chem*, 2015, **208**, 485.

5 (a) L. Zeng, E. W. Miller, A. Pralle, E. Y. Isacoff and C. J. Chang, *J. Am. Chem. Soc.*, 2006, **128**, 10; (b) S. R. Liu and S. P. Wu, *J. Fluoresc.*, 2011, **21**, 1599; (c) C. Zhou, Y. Song, N. Xiao, Y. P. Li and J. Y. Xu, *J. Fluoresc.*, 2014, **24**, 1331; (d) Y. H. Wang, C. Zhang, X. C. Chen, B. Yang, L. Yang, C. L. Jiang and Z. P. Zhang, *Nanoscale*, 2016, **8**, 5977; (e) Z. F. Xu, P. H. Deng, J. H. Li and S. P. Tang, *Sensor Actuat B-Chem*, 2018, **255**, 2095; (f) P. Samang, K. Silpcharu, M. Sukwattanasinitt and P. Rashatasakhon, *J. Fluoresc.*, 2019, **29**, 417.

6 (a) M. D. Allendorf, C. A. Bauer, R. K. Bhakta and R. J. T. Houk, *Chem. Soc. Rev.*, 2009, **38**, 1330; (b) Y. J. Cui, Y. F. Yue, G. D. Qian and B. L. Chen, *Chem. Rev.*, 2012, **112**, 1126; (c) D. Banerjee, Z. C. Hu and J. Li, *Dalton Tran.*, 2014, **43**, 10668; (d) Z. C. Hu, B. J. Deibert and J. Li, *Chem. Soc. Rev.*, 2014, **43**, 5815; (e) R. B. Lin, S. Y. Liu, J. W. Ye, X. Y. Li and J. P. Zhang, *Adv Sci.*, 2016, **3**; (f) W. P. Lustig and J. Li, *Coord. Chem. Rev.*, 2018, **373**, 116.

7 (a) Z. Hao, X. Song, M. Zhu, X. Meng, S. Zhao, S. Su, W. Yang, S. Song and H. Zhang, *J. Mater. Chem. A*, 2013, **1**, 11043; (b) B. Liu, W.-P. Wu, L. Hou and Y.-Y. Wang, *Chem. Commun.*, 2014, **50**, 8731; (c) L. Li, S. Shen, R. Lin, Y. Bai and H. Liu, *Chem. Commun.*, 2017, **53**, 9986; (d) J. A. Smith, M. A. Singh-Wilmot, K. P. Carter, C. L. Cahill and J. A. Ridenour, *Cryst Growth Des*, 2019, **19**, 305.

8 G. M. Sheldrick, *Acta Crystallogr., Sect. C: Struct. Chem.*, 2015, **71**, 3.

9 (a) N. B. Shustova, A. F. Cozzolino, S. Reineke, M. Baldo and M. Dinca, *J. Am. Chem. Soc.*, 2013, **135**, 13326; (b) Z. W. Wei, Z. Y. Gu, R. K. Arvapally, Y. P. Chen, R. N. McDougald, J. F. Ivy, A. A. Yakovenko, D. W. Feng, M. A. Omary and H. C. Zhou, *J. Am. Chem. Soc.*, 2014, **136**, 8269; (c) Z. C. Hu, G. X. Huang, W. P. Lustig, F. M. Wang, H. Wang, S. J. Teat, D. Banerjee, D. Q. Zhang and J. Li, *Chem. Commun.*, 2015, **51**, 3045; (d) B. J. Deibert, E. Velasco, W. Liu, S. J. Teat, W. P. Lustig and J. Li, *Cryst Growth Des*, 2016, **16**, 4178.

10 G. Huang, L. Yang, Q. Yin, Z.-B. Fang, X.-J. Hu, A.-A. Zhang, J. Jiang, T.-F. Liu and R. Cao, *Angew. Chem. Int. Ed.*, 2020, **59**, 4385.

11 (a) J. C. Sanchez and W. C. Trogler, *J. Mater. Chem.*, 2008, **18**, 3143; (b) J. C. Sanchez, S. A. Urbas, S. J. Toal, A. G. DiPasquale, A. L. Rheingold and W. C. Trogler, *Macromolecules*, 2008, **41**, 1237.

12 (a) G. P. Li, G. Liu, Y. Z. Li, L. Hou, Y. Y. Wang and Z. H. Zhu, *Inorg. Chem.*, 2016, **55**, 3952; (b) C. S. Cao, H. C. Hu, H. Xu, W. Z. Qiao and B. Zhao, *CrystEngComm*, 2016, **18**, 4445; (c) J. Chen, H. Y. Chen, T. S. Wang, J. F. Li, J. Wang and X. Q. Lu, *Anal. Chem.*, 2019, **91**, 4331.

13 (a) J. M. Lindquist and J. C. Hemminger, *Chem. Mater.*, 1989, **1**, 72; (b) M. Wang, B. Yuan, T. Ma, H. Jiang and Y. Li, *RSC Adv*, 2012, **2**, 5528.

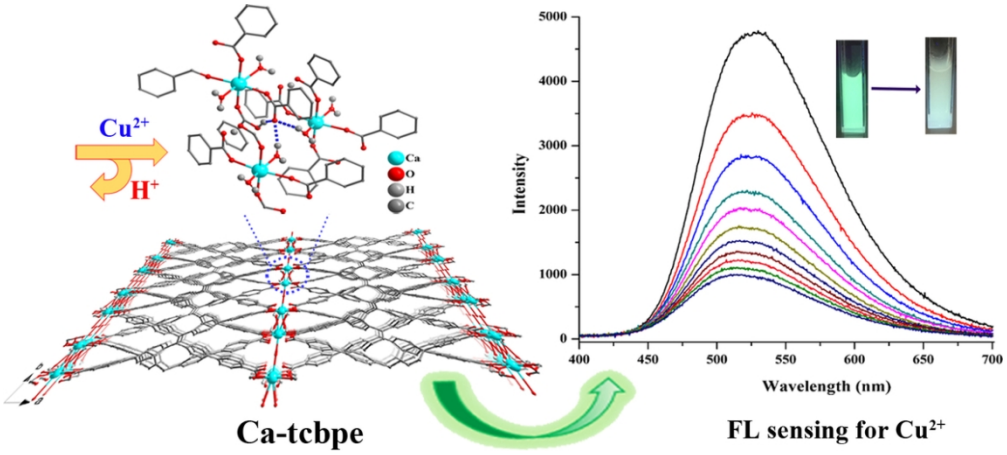

99x44mm (300 x 300 DPI)